Title

Pharmacologic modulation of nasal epithelium augments neural stem cell targeting of glioblastoma

Journal

Theranostics, 9(7)

ISSN

1838-7640

Authors

Spencer, Drew
Yu, Dou
Morshed, Ramin A
et al.

Publication Date

2019

DOI

10.7150/thno.29581

IVYSPRING INTERNATIONAL PUBLISHER

Theranostics

2019; 9(7): 2071-2083. doi: 10.7150/thno.29581

Research Paper

Pharmacologic modulation of nasal epithelium augments neural stem cell targeting of glioblastoma

Drew Spencer[1,2], Dou Yu[1,2], Ramin A. Morshed[1,3], Gina Li[2], Katarzyna C. Pituch[2], David X. Gao[1], Nicola Bertolino[4], Daniele Procissi[4], Maciej S. Lesniak[1,2], and Irina V. Balyasnikova[1,2]✉

1. The Brain Tumor Center, University of Chicago, Chicago, IL 60637, USA
2. Department of Neurological Surgery, Northwestern University at Chicago, 676 N. Saint Clair, Suite 2210, Chicago, IL 60611 USA
3. Department of Neurological Surgery, University of California San Francisco, 505 Parnassus Avenue, Rm M779, San Francisco, CA 94143 USA
4. Department of Radiology, Northwestern University at Chicago, 737 North Michigan Avenue, Suite 1600, Chicago, IL 60611 USA

✉ Corresponding author: Phone: 312.503.4868 Fax: 312.695.0225 Email: irinabal@northwestern.edu

Received: 2018.08.29; Accepted: 2019.02.11; Published: 2019.04.06

Abstract

Glioblastoma (GBM) remains the most lethal and untreatable central nervous system malignancy. The challenges to devise novel and effective anti-tumor therapies include difficulty in locating the precise tumor border for complete surgical resection, and rapid regrowth of residual tumor tissue after standard treatment. Repeatable and non-invasive intranasal application of neural stem cells (NSCs) was recently shown to enable clinically relevant delivery of therapy to tumors. Treatment with chemotactic NSCs demonstrated significant survival benefits when coupled with radiation and oncolytic virotherapy in preclinical models of GBM. In order to further augment the clinical applicability of this novel therapeutic platform, we postulate that the FDA-approved compound, methimazole (MT), can be safely utilized to delay the nasal clearance and improve the ability of NSCs to penetrate the olfactory epithelium for robust *in vivo* brain tumor targeting and therapeutic actions. METHODS: To examine the role of reversible reduction of the olfactory epithelial barrier in non-invasive intranasal delivery, we explored the unique pharmacologic effect of MT at a single dosage regimen. In our proof-of-concept studies, quantitative magnetic resonance imaging (MRI), immunocytochemistry, and survival analysis were performed on glioma-bearing mice treated with a single dose of MT prior to intranasal anti-GBM therapy using an oncolytic virus (OV)-loaded NSCs. RESULTS: Based on histology and *in vivo* imaging, we found that disrupting the olfactory epithelium with MT effectively delays clearance and allows NSCs to persist in the nasal cavity for at least 24 h. MT pretreatment amplified the migration of NSCs to the tumor. The therapeutic advantage of this enhancement was quantitatively validated by tissue analysis and MRI tracking of NSCs loaded with superparamagnetic iron oxide nanoparticles (SPIOs) in live animals. Moreover, we observed significant survival benefits in GBM-bearing mice treated with intranasal delivery of oncolytic virus-loaded NSCs following MT injection. Conclusion: Our work identified a novel pharmacologic strategy to accelerate the clinical application of the non-invasive NSCs-based therapeutic platform to tackle aggressive brain tumors.

Key words: neural stem cells, intranasal delivery, glioblastoma, clearance, barrier

Introduction

The dismal prognosis of glioblastoma (GBM) and the continued lack of effective therapies demand innovation in novel treatment options. Currently, the standard of care consists of surgical resection in addition to temozolomide (TMZ) and radiation, which provide a survival benefit of only 6-8 months compared to surgical resection alone [1]. Moreover, recurrent GBM is more aggressive and almost uniformly fatal. Resistance to treatment is profound both at the time of diagnosis and after initiation of therapy [2, 3]. A major challenge for developing effective anti-GBM therapies is the severe limitation on targeted therapeutic delivery to tumor sites. The development of innovative methodologies aiming to

effectively deliver new and existing therapeutics specifically to the malignant tissue are in urgent demand. Novel strategies must be implemented to shuttle therapeutics across the blood-brain barrier (BBB) to reach the adequate dosage accumulation in a poorly vascularized tumor mass.

The intranasal (IN) route of administration of therapeutics to target CNS pathology has become a rapidly growing focus of research, offering many potential benefits in the therapeutic delivery of anticancer agents. As a non-invasive route with strong potential for sustained and readily adjustable therapy, IN delivery has already demonstrated favorable efficacy and safety profiles for a variety of medical conditions [4, 5]. The IN delivery of therapeutics utilizes the unique nasal anatomy to improve targeted brain delivery through three routes of absorption: the olfactory nerves, the trigeminal nerves, and the nasal lymphatics/vasculature [4]. The nasal epithelium provides a direct connection to the olfactory bulb via the olfactory nerves across the cribriform plate, which bypasses the BBB and provides access to the limbic cortex and deep regions of the brain. The V1 and V2 branches of the trigeminal nerves innervate portions of the nasal cavity and provide a direct path to the pons and thalamus. Interestingly, the presence of stem cells in the olfactory bulbs and trigeminal nerves of mice after IN delivery has been recently documented, suggesting that stem cells can enter the brain via both routes [6, 7]. Finally, the nasal cavity is well-vascularized and might allow for direct entry of therapeutics into the circulation and then through the BBB into brain tissue.

Given these advantageous properties for therapeutic distribution in the brain, IN therapy has recently been explored for GBM [6, 8]. The IN delivery of stem cell carriers is of particular interest in GBM due to the tumor tropism and low immunogenicity of stem cells [9, 10]. The delivery of mesenchymal stem cell-based therapy via the IN route has previously been shown to be efficacious in models of GBM [8]. However, improving the efficiency of migration presents a continued challenge, as previous reports have shown that only a small fraction of stem cells reach the tumor [6, 8].

The brain targeting of therapeutic stem cells via IN delivery can be improved through temporary modifications to the nasal epithelium. The epithelium presents a multi-functional physiological barrier to substances entering the nasal cavity, most critically pathogens. The layered epithelium and junctions between the epithelial cells prevent the transmission of substances based on size, composition, and presence of a specific transporter. The apical nasal epithelia are also ciliated, another mechanism of clearing harmful pathogens from the body. Thus, balancing the permissive entry of desired agents with the adequate protection of the patient from harmful side effects or disease becomes the key challenge in devising effective IN delivery strategies.

In this study, we investigated two different strategies to enhance the efficiency of IN stem cell migration to GBM: the use of fibrin sealant (e.g., fibrin glue) to delay nasal clearance, and the administration of methimazole (MT) to reduce the thickness of the olfactory epithelium. Fibrin sealant is fibrin- and thrombin-based biodegradable glue clinically used in a variety of surgical applications, including neurosurgery. We sought to mechanically delay the rapid clearance of NSCs by ciliated epithelium from the nasal cavity using fibrin glue. MT is an FDA-approved medicine for hyperthyroidism with a unique side effect of temporary and reversible olfactory epithelium depletion [11, 12]. We sought to harness this particular side effect to prevent the clearance of NSCs from the nasal cavity and disrupt the barrier to olfactory nerve endings by administering MT before the IN delivery of stem cells. The terminally differentiated pseudostratified columnar apical epithelium of the nasal cavity is affected by MT, with preservation of the basal and horizontal stem-like cell layers [13]. The nasal epithelium is markedly depleted within the first 72 h and fully regenerates after approximately 7 days, although the thickness and architecture can remain abnormal for up to a month [13].

Here, we demonstrate that fibrin glue is able to delay the clearance of NSCs from the nasal cavity transiently. On the other hand, MT more durably improves the persistence of NSCs in the nasal cavity, consequently improving NSCs migration to tumor xenografts. Most importantly, we demonstrate that the improved penetration of NSCs to the brain confers a significant improvement in the survival of mice bearing GBM using IN delivery of oncolytic adenovirus (OV)-loaded NSCs. To our knowledge, this is the first report that attempts to optimize the IN delivery of stem cells to GBM via pharmacologic manipulation of the nasal epithelial barrier.

Materials and Methods

Cell culture

HB1.F3.CD human neural stem cell (NSC) line was graciously provided by Dr. Karen S. Aboody (City of Hope National Medical Center and Beckman Research Institute, Duarte, CA). HB1.F3.CD cells were modified to express either green fluorescence protein (GFP) or firefly luciferase (fluc) via lentiviral transduction, designated in the text as NSCs-GFP or

NSCs-fluc, respectively. U87MG glioma cell line was obtained from ATCC. Patient-derived GBM43 glioma xenograft line was kindly provided by Dr. David James (Northwestern University, Chicago, IL). All cell lines were maintained in Dulbecco's Modified Eagle Medium (DMEM, Life Technologies, Grand Island, NY) supplemented with 10% fetal bovine serum (Hyclone, Logan, UT) and 1% penicillin/streptomycin (Invitrogen, Carlsbad, CA) in a humidified 5% CO_2 atmosphere at 37 ^oC.

NSC labeling with SPIOs. NSCs were grown in a T75 cm^2 flask (BD Biosciences, San Diego, CA) to about 80% confluency. NSCs were labeled with micron-size paramagnetic iron oxides (SPIOs) at 20 particles/cell (Bangs Laboratories, Fishers, IN) as we previously described in reduced serum Opti-MEM medium (Life Technologies, Grand Island, NY) [8]. After a 4 h incubation in a humidified 5% CO_2 incubator at 37 ^oC, the Opti-MEM medium with excess SPIO was aspirated and replaced with DMEM media containing 10% FBS.

NSC loading with OV. NSCs were previously modified to overexpress C-X-C chemokine receptor type 4 (CXCR4), which has been shown to facilitate the successful migration of NSCs to the brain [14]. NSCs were grown in a T75 cm^2 flask (BD Biosciences, San Diego, CA) to about 80% confluency. NSCs were then loaded with the oncolytic virus CRAd-S-pK7 at 10 or 50 viral particles (vp) per cell using a previously published protocol [9]. These NSCs are referred to as NSCs-OV and were utilized *in vitro* and in the survival study.

Animal studies

All animal studies were approved by the Institutional Committee on Animal Use at the University of Chicago or Northwestern University. Six to eight-week-old male athymic nude mice were obtained from Harlan Laboratories (Indianapolis, IN) and maintained in a barrier facility at the University of Chicago or Northwestern University. All surgical procedures were completed in accordance with NIH guidelines on the care and use of laboratory animals for research purposes. Intracranial xenografts were established in the right frontal lobe as previously described [8].

Animals assigned to fibrin glue experimental groups were given 3 µL of fibrin glue via IN injection immediately following NSCs administration. Fibrin glue was modified as follows: the thrombin part of fibrin sealant was diluted to 5U/mL in order to achieve a delay of about 30 s in the formation of the fibrin sealant after mixing the two reagents.

Animals assigned to MT experimental groups were given intraperitoneal (i.p.) injections of 50 µg/g MT (Sigma-Aldrich, St. Louis, MO) in 100 µL of sterile phosphate buffered saline (PBS) 48 h prior to NSCs administration.

Administration of NSCs was performed for all studies as follows: mice were anesthetized with an i.p. injection of 0.2 ml of a stock solution containing ketamine HCl (25 mg/mL), xylazine (2.5 mg/mL), and PBS (Hyclone, Logan, UT) and placed in the supine position. NSCs were inoculated into the nasal cavity in 3 separate 4 µL aliquots at 5 min intervals, totaling $5x10^5$ cells.

Bioluminescent imaging (BLI) of NSCs **in vivo.** NSCs-fluc in the nasal cavity were detected using the Xenogen IVIS 200 system (Perkin-Elmer, Waltham, MA). Mice were injected i.p with 150 µL (4.5 mg) of D-luciferin sodium salt (Gold Biotechnology, St Louis, MO). An additional 3 µL was placed in each nostril to assist with the detection of cells. Animals were imaged 10 min later, allowing for D-luciferin circulation and uptake, with the signal recorded in photon counts. The localization of NSCs-fluc in the nasal cavity was analyzed at 0, 6 and 24 h after injection. Calculations were performed by drawing the region of interest (ROI) and measuring of the normalized luminescent signal within ROI for each assessed time point.

Administration of NSCs-fluc to investigate persistence in the nasal cavity. Animals without tumors were separated into control, fibrin glue, and MT groups (n=5). All animals were inoculated with NSCs-fluc via IN delivery, as described above. Experimental groups were treated as described above. Control mice received 100 µL of PBS via i.p. injection. Live BLI was used to assess the survival and persistence of NSCs in the nasal cavity at 0, 6, and 24 h after inoculation.

Administration of SPIO-loaded NSCs to track migration towards glioma xenografts. U87MG or GBM43 intracranial xenografts were injected and allowed to engraft. Animals were separated into control and MT groups. Experimental MT groups were treated as described above. Control mice received 100 µL of PBS via i.p. injection. Mice were euthanized 48 h following SPIO-loaded IN NSC inoculation, and sagittal and axial sections were prepared for Prussian blue staining, as described below.

Administration of NSCs-GFP to track migration towards patient-derived GBM43 xenografts. GBM43 glioma cells were injected intracranially and allowed to grow for at least 7 days. Animals were separated into two groups and treated either with PBS or MT as described above. In 48 h, NSCs-GFP were introduced in animals via IN delivery, and the mice were euthanized two days later. Sagittal and axial sections were prepared for histological analysis and

fluorescent microscopy as described below.

Survival study. In order to understand if an increase in the number of NSCs migrating to glioma tumors after MT treatment translates to survival advantage, we loaded NSCs with CRAd-S-pK7 oncolytic virus, the approach well established in our previous studies [9, 15]. Animals were separated into control, NSCs-OV, and MT+NSCs-OV groups (n=8). Five days after intracranial injection of GBM43 glioma cells, the MT+NSCs-OV experimental group was administered MT as described above. Control and NSCs-OV mice received 100 µL of PBS via i.p. injection. IN treatments with either PBS or NSCs-OV were carried out 48 h following MT injection. This treatment regimen was repeated once a week twice; i.e., experimental mice received three IN treatments of NSCs-OV. The animals were followed for neurological symptoms consistent with NIH guidelines and euthanized at the appropriate endpoints. No adjuvant therapy was utilized in addition to our experimental therapy.

MRI acquisition

Eight mice bearing GBM43 xenograft tumors were divided into three cohorts: control (n=2), NSCs+saline (n=3) and NSCs+MT (n=3). All mouse cohorts were scanned at baseline (pre-treatment with NSCs) and 24, 48, and 120 h post-treatment with NSCs. During MRI, animals were anesthetized using isoflurane mixed with 100% O_2 (1.5-2% concentration). The MRI acquisitions were performed using a 7 Tesla MRI scanner (ClinScan, Bruker) operated with the Syngo MR VB15 user interface (Siemens) and equipped with a 12-cm gradient (strength 290 mT/m and slew rate 1160 T/m/s). We employed a cross-coil configuration with a 4-channel receiver mouse head surface coil and a quadrature transmitter volume coil. The imaging protocol included a localizer, 3 2D-TSE (turbo spin echo) oriented along the three main axes (coronal, axial and sagittal; TR/TE = 1560/40 ms; voxel size = 0.074x0.074x0.7 mm^3) for morphological references and a 3D-FLASH-MGRE (fast long angle shot multi-gradient echo; TR = 40 ms; TEs = 2.51, 6.04, 9.57, 13.1 ms; flip angle = 15; averages = 6; matrix = 152x256x44; voxel size = 0.15x0.15x0.16 mm^3) for measurement of T2*.

Image Analysis

The region of interest (ROI) delineations were performed using ITK-SNAP vs. 3.6.0 software and custom MatLab (R2017a) scripts. For anatomical reference, we generated an average image from the four echoes images. This image was used to generate binary brain-masks and tumor ROIs employing a semi-automated thresholding delineation algorithm (ITK-SNAP). After applying brain-masks to each 3D-FLASH-MGRE image, we computed whole-brain T2* and R2* maps. Finally, the mean R2* values were extracted from tumor ROIs for all R2* relaxation time maps.

Histology, fluorescent microscopy, and confocal microscopy

Preparation of sagittal and axial sections. To analyze the distribution of NSCs in the nasal cavity and their migration across the cribriform plate to xenograft tumors, we performed sagittal section preparations to expose the nasal epithelium. Mice were perfused with 5 mL of 4% paraformaldehyde (PFA) in 0.1 M phosphate buffer. Whole mouse heads were then post-fixed in 4% PFA overnight at 4 ^oC and then dehydrated in 30% sucrose solution for 24h. The skin, jaw, and cranium were dissected away to expose the whole brain and nasal cavity, which was then embedded in OCT compound (Sakura Finetek USA, Inc., Torrance, CA), divided along the midline using a TechniEdge razor blade (IDL Tools, Kenilworth, NJ) and preserved at -80 ^oC until cryosectioning. Sagittal sections (10 µm thick) were collected on a Microm cryostat (Model HM505E, Leica Biosystems, Buffalo Grove, IL). To analyze the migration of NSCs toward and their coverage of xenograft tumors, we prepared axial sections (10 µm) of mouse brains. Brain tissue was collected after perfusion as described above, and all fixed brain tissues were embedded, cryosectioned, and mounted on slides for histological (H&E) and fluorescent microscopic analyses.

Detection of SPIOs. All chemicals were acquired from Sigma-Aldrich (St. Louis, MO) unless noted otherwise. NSCs labeled with SPIOs were visualized with Prussian blue staining according to previously published work [8]. Frozen 10 µm fresh brain sections were fixed in 4% PFA for 10 min, washed thrice in PBS, stained with potassium ferrocyanide trihydrate, and counterstained with a nuclear Fast Red stain (Vector Laboratories, Burlingame, CA) [8]. Digital image files were created with a 3D Histech Pannoramic Scan whole slide scanner (Perkin Elmer, Waltham, MA) utilizing a Zeiss AxioCam MRm CCD camera (fluorescence) (Carl Zeiss Microscopy, Thornwood, NY). Individual images were compiled with the 3D Histech Pannoramic Viewer software (Perkin Elmer, Waltham, MA).

Confocal microscopy. GBM43/NSCs-GFP tissue specimens were visualized via confocal microscopy using blue (405 nm) and green (488 nm) excitation lasers to obtain representative images of tumors and tumor-tropic NSCs-GFP cells. Three brains of animals per group were frozen and sectioned. Images were

captured and processed (20 observations per group) with a 3i Marianas Yokogawa-type spinning disk confocal microscope employing an Evolve EM-CCD camera (Photometrics, Tucson, AZ) running on SlideBook v5.5 software (Intelligent Imaging Innovations, Denver, CO) at the Integrated Microscopy Core Facility at the University of Chicago.

Cytotoxicity assay. The dose-effect of MT on the viability of NSCs, U87MG glioma cell line or patient-derived xenograft, GBM6 and GBM43, lines was assessed using standard XTT (Roche Diagnostics) assay per manufacturer's protocol. A trypan blue exclusion method has been utilized to determine the effect of concurrent treatment with MT and OV on the viability of GBM43 cells *in vitro*.

Quantification of NSCs tumor-tropic migration. Serial sections of GBM43/NSCs-GFP tissue specimens were analyzed. Ten high power (20X) image fields per mouse were randomly selected and analyzed. The GFP and hNestin (red) signals visualizing NSCs and GBM43 glioma cells, respectively, were quantified in each digital image based on uniform intensity ranges determined against background signal levels using the histogram function in Adobe Photoshop™ software (Adobe Systems Inc., San Jose, CA). Unbiased comparisons were done using 30 digital images collected from three animals per treatment group.

Evaluation of intratumoral delivery of viruses by NSCs. Five days post IN delivery of NSCs loaded with OV, animals were euthanized and brain tissue processed for analysis. Viral payload was determined by hexon fluorescent staining as previously described [14]. Quantification of mean fluorescence intensity (arbitrary units, AU) of DAPI and hexon signal was done using Image J Software (NIH, Bethesda, Maryland) [16]. The intensity of the hexon signal was normalized with the intensity of the DAPI signal. Three fields per section, of six sections (n=6) for each of the three animals (n=3) in both experimental groups, with or without MT, were analyzed.

Statistical considerations

All statistical analyses were performed using GraphPad Prism 4 (GraphPad Software Inc., San Diego CA). Differences among groups were evaluated using either parametric or nonparametric Student's *t*-test or two-way analyses of variance, followed by post hoc correction as appropriate. For the *in vivo* data, survival curves were generated via the Kaplan–Meier method, and a log-rank test was applied to compare the distributions of survival times. All reported *p* values were two-sided and were considered to be statistically significant at $p<0.05$.

Results

Fibrin glue and MT treatments prolong the persistence of NSCs in the nasal cavities of mice.

In our studies, we explored two strategies to enhance IN delivery of therapeutic NSCs to glioblastoma through (i) the administration of fibrin glue to seal stem cells over the nasal epithelia, and (ii) the delivery of MT to decrease the thickness of the epithelial barrier (Figure 1). NSCs presence in the nasal cavity was detectable in animals of both treatment groups within 30 min (0 h) after IN administration of fluc-expressing NSCs as measured by BLI. However, a time-dependent decrease in the number of cells present was evident at 6 and 24 h. Scaled images were compared for control, fibrin glue and MT groups, with radiance as the qualitative measure of the number of surviving cells. Fibrin glue was found to have a small positive effect on the persistence of NSCs-fluc after IN injection when

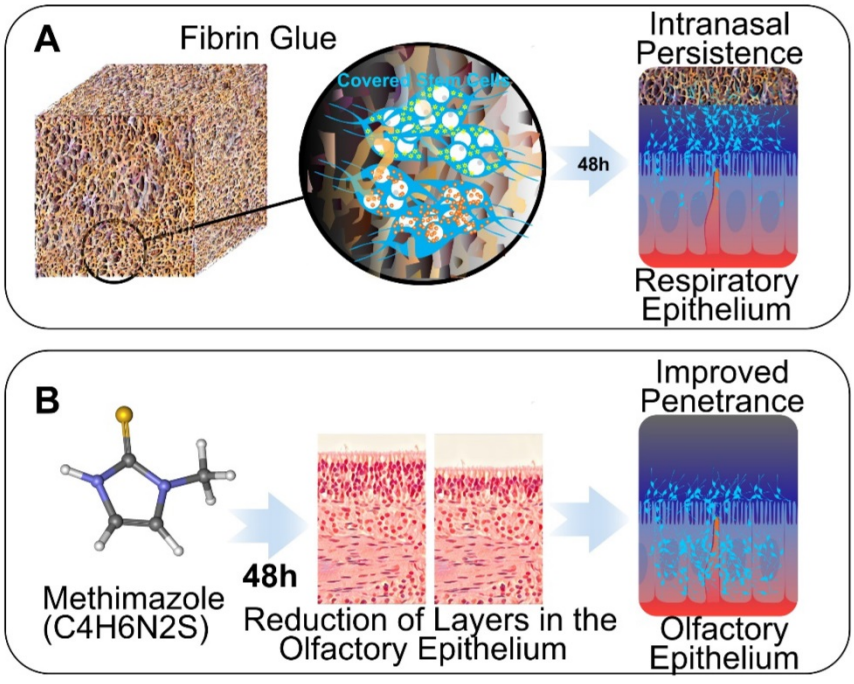

Figure 1. Schematic of strategies to enhance IN delivery of therapeutic neural stem cells (NSCs) to glioblastoma. A, The biocompatible 3 dimensional structure of fibrin glue is utilized to seal NSCs in a nasal cavity to delay clearance and enhance persistence. **B**, The effect of MT on the disruption of the olfactory epithelium barrier is utilized to improve the brain entry of NSCs through olfactory route.

compared to the control treatment. Fibrin glue-treated mice exhibited a higher radiance at 6 h than in control animals with no discernible difference at 24 h (Figure 2 A-C). However, a significantly improved persistence of NSCs was observed in the MT group as compared to the control mice at both 6 and 24 h post IN treatment (p<0.001, Student's t-test). The difference at 24 h was remarkable in MT-treated animals, with radiance at ~10^7 compared to at ~10^3 in both control- and fibrin glue-treated animals. Given that MT was found to significantly increase the persistence of NSCs within the nasal cavity for 24 h when compared to both the fibrin glue and control groups, the pretreatment with MT was selected as the key strategy for enhancing the delivery of NSCs to the brain via the IN route in all subsequent experiments.

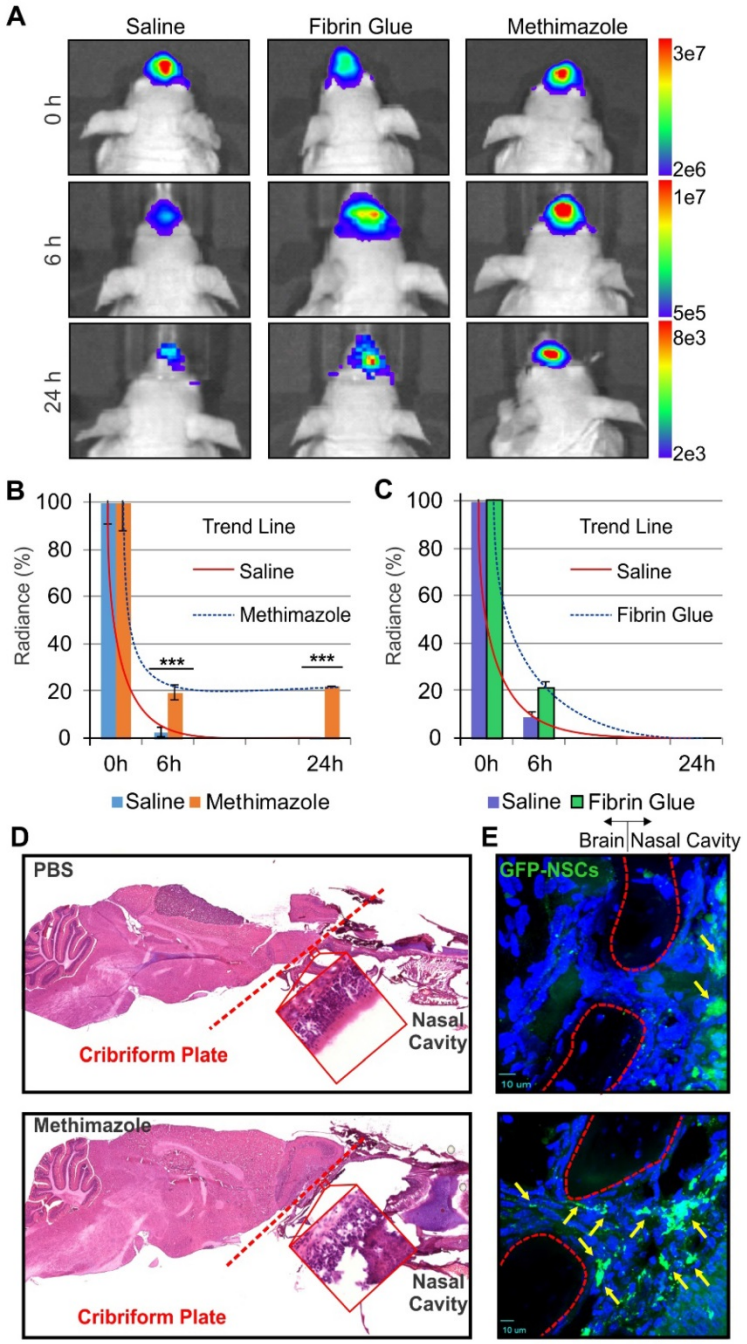

Figure 2. The effect of MT and fibrin glue treatments on the persistence of NSCs in the nasal cavity of mice. A, Representative BLI images of animals after IN delivery of NSCs-fluc from each of the treatment groups (PBS control, fibrin glue, and MT). **B**, Quantitative measurements of the persistence of NSCs-fluc in the nasal cavity after MT treatment (n=5, ***p<0.001, Student's t-test). **C**, Quantitative measurements of the persistence of NSCs-fluc in the nasal cavity after fibrin glue treatment (n=5, ***p<0.001, Student's t-test). **D**, Sagittal sections of representative mouse brains bearing U87MG tumors in PBS control (top) and the MT group (bottom) with the cribriform plate (red dashed lines) shown, delineating the olfactory bulbs and the nasal cavity. Histology confirms that MT induces disruption of the olfactory epithelium (red boxes). **E**, Fluorescent microscopy images of the cribriform plate area (red dashed outline indicates areas where DAPI does not stain calcified bone structure) show improved migration of NSCs-GFP (green cells and yellow arrows) from the nasal cavity to the brain, as compared with non-treated group.

MT treatment in mice compromises the integrity of the olfactory epithelial barrier between the nasal cavity and brain.

It has been previously reported that treatment of mice with MT disrupts differentiated cells of the olfactory epithelium [12, 17]. Therefore, we aimed to determine if changes induced in the nasal epithelium by MT administration also affect the ability of NSCs to migrate from a nasal cavity to the brain through the cribriform plate. The integrity of nasal epithelium over the cribriform plate was compared in control and MT-treated mice using H&E staining and confocal microscopy. Indeed, MT treatment induced the depletion and sloughing of the nasal epithelium (Figure 2 D). This was demonstrated by the presence of gaps between cells and loss of the typical epithelial pseudostratified columnar architecture, whereas the basal layer comprised of horizontal and round stem cells was morphologically intact. Confocal, high-power images of the cribriform plate in the nasal cavity demonstrated that GFP-expressing NSCs were mostly present near the basal layer or basement membrane of the epithelium in control mice in 48 h after IN treatment with NSCs. In MT-treated animals, NSCs-GFP were observed traversing the cribriform plate along the path of the olfactory nerves (Figure 2E).

MT does not affect the survival of mice bearing intracranial GBM43 PDX tumor.

MT treatment causes robust damage to olfactory epithelium within the first 24 h after treatment [11]. Therefore, we aimed to understand if MT also directly affects the viability of glioma cells or NSCs (carriers of the oncolytic virus to glioma tumors). All three glioma cell lines and NSCs were treated *in vitro* with MT at 0-500 µg/mL for 24 h. The viability of cells was evaluated by an XTT assay. Figure 3A shows that MT is not toxic to either NSCs or other glioma cells at any tested concentration, while GBM43 cells are more sensitive to MT treatment. A statistically significant decrease in the viability was observed after treatment with 31-500 µg/mL of MT (p<0.0001, two-way ANOVA), but not in the 0-31 µg/mL concentration range.

Next, we assessed whether MT increases the response of GBM43 cells to the oncolytic activity of CRAd-S-pK7 in GBM43 cells. The concentration of MT at 60 µg/mL is similar to Cmax in mice treated with a single i.p. a dose of MT at 50 µg/g of body weight [11]. Therefore, this dose was chosen for the experiment. Although dose-dependent toxicity was observed in GBM43 cells (p<0.0001, two-way ANOVA) due to replication of the oncolytic virus, CRAd-S-pK7, in agreement with our previous studies [9], concurrent treatment with MT did not affect the oncolytic activity of the virus in GBM43 cells (Figure 3 B).

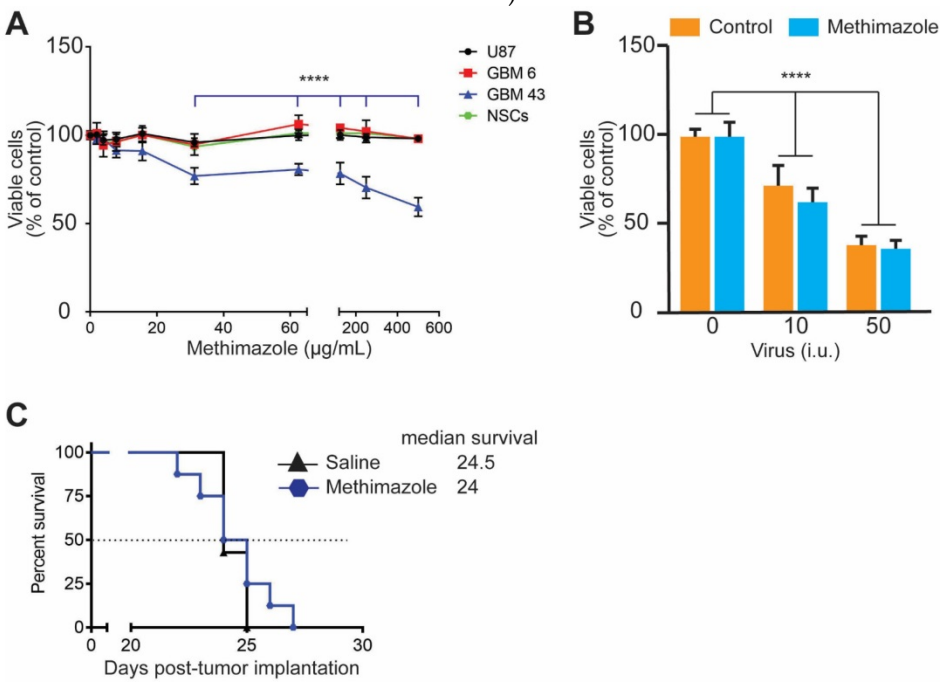

Figure 3. The effect of MT on the viability of glioma cells *in vitro* and *in vivo*. A, U87MG (p≥0.05), GBM6 (p≥0.05), GBM43 glioma cells (****p<0.0001) and NSCs (p≥0.05) were treated with MT at 0-500 µg/mL for 24 h. The viability of cells was measured using an XTT assay. Data presented as mean±SD, n≥4, two-way ANOVA. **B**, Oncolytic properties of CRAd-S-pK7 were evaluated in the presence of MT at 60 µg/mL. GBM43 cells were infected at 10 and 50 infectious units (i.u.) of virus per cells, n≥4, ****p<0.0001 and p≥0.05 for the oncolytic activity of virus alone and in the presence of MT respectively; two-way ANOVA. **C**, Mice bearing GBM43 PDX glioma tumors were treated with a single i.p. injection of saline or MT at 50 µg/g of body weight 5 days after tumor implantation. The survival of animals was recorded and analyzed using a log-rank test (n=7 per group).

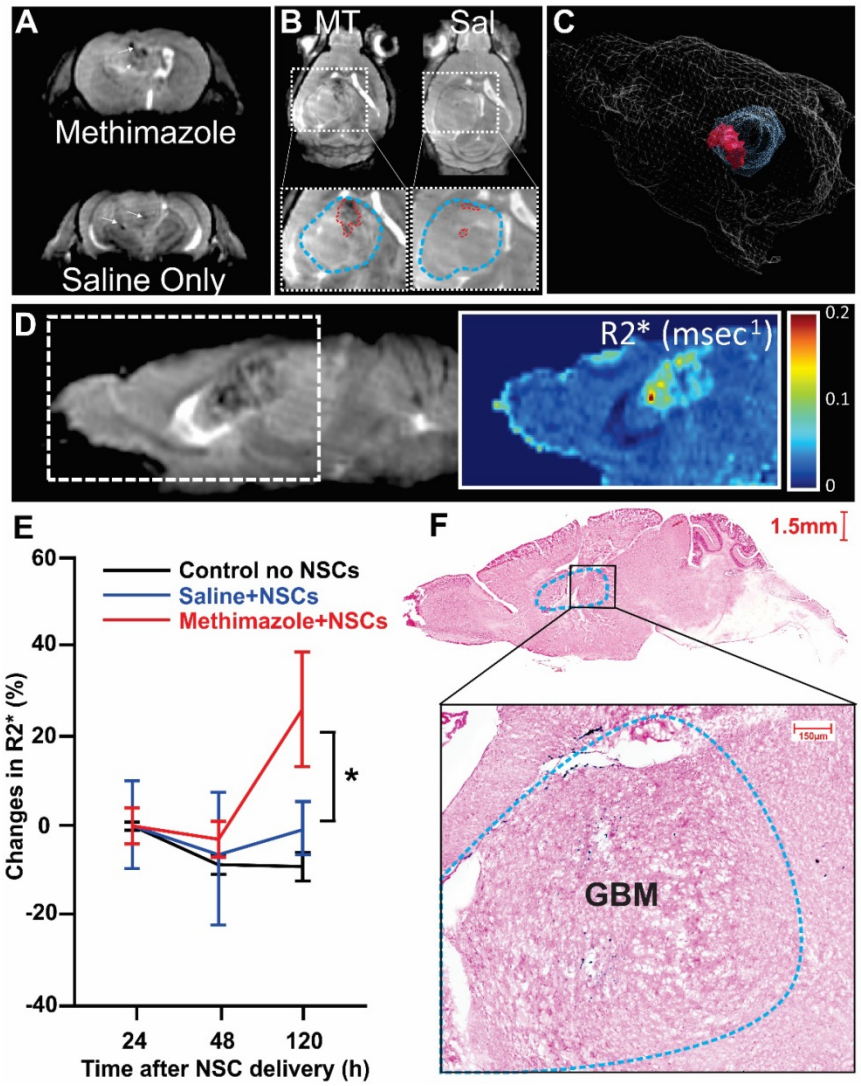

Figure 4. Magnetic Resonance Imaging (MRI) tracking NSCs' tumor infiltration. A, Representative MRI slice of an MT-treated mouse and a Saline (Sal) control at 120 h post administration. **B**, MT+NSCs shows the drastic localized decrease in signal hyperintensity within the tumor as compared to Sal+NSCs (white arrows and red dashed lines outlining the possible accumulation of labeled NSCs in blow-up inset figure which also depicts the outline of tumor region in blue). A small decrease in tumor signal is also observed in a control saline-treated group which is likely reflective of less efficient homing of NSCs. **C**, 3D rendered image of a representative MT+NSCs mouse head outline, with a superimposed three-dimensional morphometric depiction of the tumor (Blue) and of the region within the tumor with NSCs accumulation (red). **D**, A representative MR sagittal slice for one of the MT+NSCs mice is also shown alongside the corresponding R2* map. High R2* regions correspond to accumulated SPIOs. **E**, Plot showing the average R2* from each group at each time point extracted from tumor region ($p<0.05$, n=3, two-way ANOVA). **F**, Representative sagittal section of the MT-treated mouse brain, (enlarged from the boxed region of F), shows tumor mass (blue dashed outline) and the NSCs (blue dots) shown after Prussian blue staining.

Finally, in the next set of experiments, we assessed whether treatment with a single dose of MT affects the survival of animals bearing GBM43 intracranial tumors. Mice bearing GBM43 tumors were treated with a single i.p. injection of MT at 50 µg/g of body weight, a concentration shown to achieve an effective disruption of the nasal epithelium (Figure 2D). The log-rank test analysis shows that there is no difference between the control and MT-treated groups of mice in survival (Figure 3C). Collectively, these data show the lack of MT-induced toxicity *in vitro* and *in vivo* at a concentration comparable to plasma Cmax reported in wild-type mice [11].

MT treatment enhances the migration of NSCs towards intracranial glioma xenografts.

We used magnetic resonance imaging (MRI) to quantify the effect of MT treatment on the migration of SPIO-loaded NSCs by acquiring 3D whole anatomical and R2* brain images. We observed significant localized decreases in signal intensity and corresponding increases in R2* values in all mice treated with MT, reflective of the presence of SPIO's (Figure 4A, white arrows). The changes in R2* were minimal in the mouse brains administered with NSCs only and utterly absent in the control group (Figure 4B). The distribution of SPIO-induced signal (areas of

increased R2* are depicted in red) is also shown in the 3D rendering of a representative animal from the MT group (Figure 4C). This 3D depiction also shows the morphometry of the tumor (depicted in blue). A sample MRI R2* map generated from the MRI data is shown on the right of the corresponding anatomical image in Figure 4D. Quantification of SPIO-labeled NSCs accumulation in tumor xenograft was achieved by averaging for each group the R2* values extracted from the tumor region and plotting these values as a function of time after treatment (Figure 4E). The longitudinal quantitative analysis of R2* signals demonstrated that accumulation of NSCs in tumor tissue is significantly higher in MT-treated animals as compared with saline-treated control mouse brains (Figure 4E; $p<0.05$, two-way ANOVA) and is maximal at 120 h after administration. These findings were corroborated with a pattern of Prussian blue (Figure 4F) stain, which confirmed the presence of SPIO-labeled NSCs in the tumor and peri-tumoral regions as indicated by MRI. A negligible number of stained particles were noted in other regions of the brain. Thus, these findings further supported our hypotheses.

In order to further validate our findings, we next examined sections of brains with GBM43 glioma xenografts from animals treated with IN NSCs-GFP. We compared the NSCs' migration to xenograft tumors between the control and MT treated groups at 48 h after NSCs inoculation. The GFP signal was increased in the tumor and peritumoral regions in animals of the MT treatment group (Figure 5A & B) representing improved migration following the remodeling of the epithelial barrier. The GFP signal was nearly four times higher in the MT treatment group as compared with the control group (Figure 5C, $p<0.05$, Student's *t*-test). This effect was not a result of the difference in tumor size, as the hNestin signal (a predominant marker of tumor cells *in vivo*) was not significantly different between the two groups. These findings confirm that a marked increase in NSCs migration to intracranial patient-derived xenograft tumors is achievable with MT treatment of the olfactory epithelium.

IN-delivered NSCs loaded with oncolytic virus significantly improve survival in MT-treated animals

Our experiments show that the disruption of the epithelial barrier promotes the migration and accumulation of NSCs within intracranial GBM xenografts. We, therefore, examined if this could translate into an improved delivery of the anti-tumor OV payload by NSCs and achieve enhanced therapeutic benefit. The staining of brain tissue sections for the expression of the hexon viral protein revealed a significantly higher presence of OV in glioma tissue after pre-treatment of animals with MT (Figure 6A, $p<0.001$, Student's *t*-test). The quantitative analysis confirmed a significantly increased signal in the MT group as compared to control (Figure 6B). Finally, the therapeutic efficacy was assessed in mice

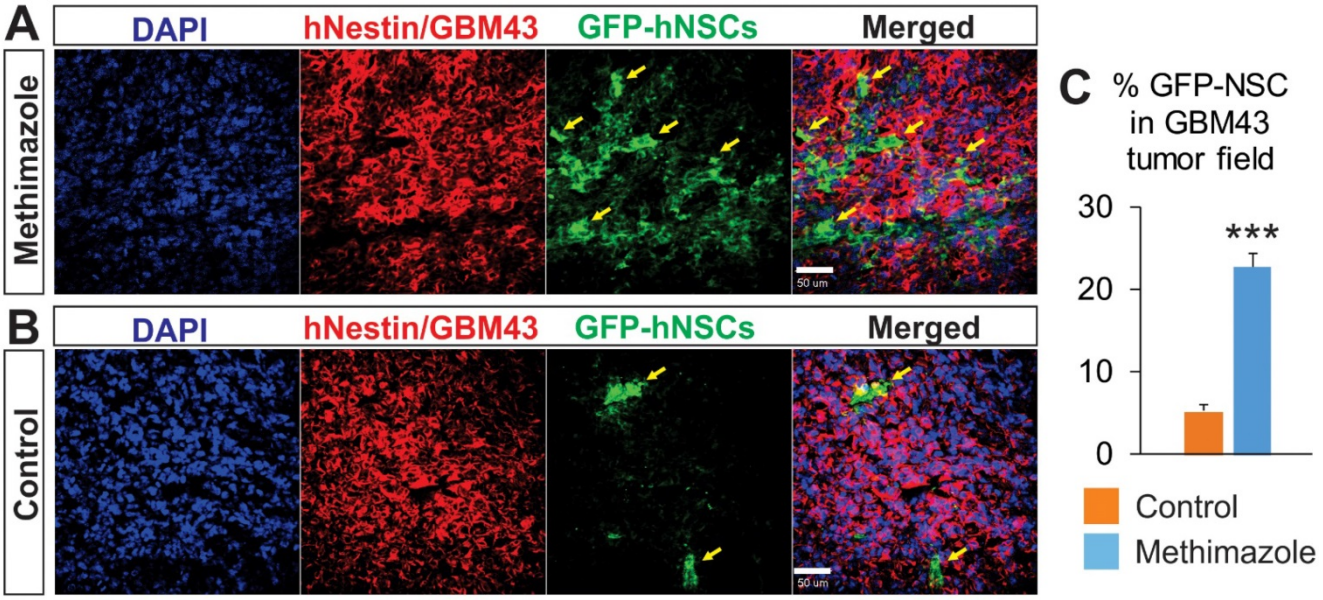

Figure 5. Analysis of the tumor tissue for the presence of NSCs after IN delivery in control and MT-treated groups. Using confocal microscopy, the presence of NSCs-GFP (green) in human GBM43 xenografts stained for hNestin (red) was analyzed to assess the ability of IN delivered NSCs to reach the tumor burden. The NSCs-GFP (green) that migrated to the tumor site were quantified based on the relative percentage of pixels shown as green over the total pixels shown as red per visual field. Significantly higher relative densities of NSCs-GFP are seen in (**A**) the brain tissue of MT-treated mice than those in (**B**) control, PBS-treated mice. **C,** ***$p<0.001$, Student's *t*-test).

with aggressive intracranial patient-derived GBM43 glioma xenografts. We observed a median survival of 23 days in the control group, and treatment with NSCs-OV alone did not significantly prolong the survival of animals (extension of the median survival of 0.5 days). However, animals in the MT+NSCs-OV group survived significantly longer to a median of 28 days (Figure 6B; 5-day extension, $p<0.05$, log-rank test). These data confirm our hypothesis that the depletion of olfactory epithelium using MT prior to IN delivery improves migration of therapeutic NSCs to tumors, increases OV dosage delivered to the tumor, and prolongs the survival of animals with aggressive GBM xenografts.

Discussion

Despite the abundant investigations for actionable treatment mechanisms and translational therapies, GBM remains a fatal disease with no cure. The complex pathogenesis and genetic evolution of GBM enable evasion from various treatment modalities that underlie its aggressive recurrence. Over a decade ago, stem cells emerged as promising vehicles for GBM therapy due to their intrinsic tumor tropism and the ability to deliver therapeutics while shielding the cargo from systemic immune responses [10]. NSCs used in our studies have been shown to be safe in GBM patients [18]. We have also demonstrated in our preclinical studies that NSCs can effectively deliver oncolytic virotherapy upon local injection in brain tumor xenografts, resulting in survival benefit in mouse models of GBM [9, 19]. Currently, this therapeutic modality is being evaluated in patients with newly diagnosed GBM in phase I clinical study (NCT03072134). We have also actively explored the IN delivery route for stem cell therapeutics due to its potential for repeatable non-invasive treatments. We have shown that stem cells are capable of delivering therapeutically effective anti-glioma treatments via the IN route, which synergizes with radiation therapy, a key component of GBM standard of care [8]. However, in these studies, we observed swift clearance of stem cells from the nasal cavity. Given that the therapeutic potency hinges largely on the level of stem cell arrival at the tumor loci, we hypothesize that strategies delaying stem cell clearance and improving persistence in the nasal cavity improve the level of stem cell migration across the epithelium to penetrate the brain parenchyma and tumor mass. Beyond its primary functions of relaying sensory information while filtering, warming, and humidifying air entering the nasal cavity, the nasal epithelium also stands as a key barrier to prevent infectious pathogen entry to the intracranial compartment [20]. The epithelial barrier also prevents the entry of environmental and other toxins via the secretion of thick mucus and the coordinated motile cilia movements to regularly remove foreign substances, passing on mucus over the course of several days [20]. Due to the extended time that stem cells need to traverse the nasal epithelium, stem cell-based therapeutics are severely limited by nasal clearance. Thus, in this study we explored the strategy of delaying clearance of stem cells using two FDA approved compounds, fibrin glue and MT, to promote the migration of NSCs to tumor xenografts and delivery a potent therapeutic payload (Figure 1).

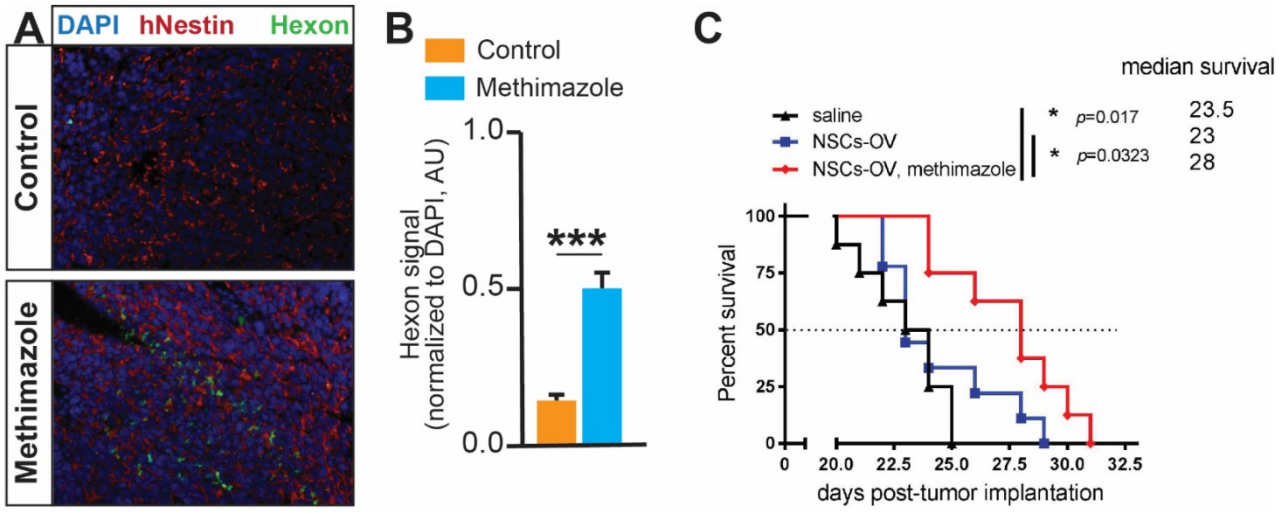

Figure 6. Disruption of the nasal epithelial barrier improves the survival of animals after IN delivery of NSCs loaded with OV. A, Representative images of GBM43 tissue sections from the brain of mice which received IN OV-NSCs therapy. GBM43 is visualized by staining for hNestin (red), whereas viral protein is visualized by staining for hexon protein (green). Nuclei of cells are visualized by DAPI (blue). **B,** Quantification of hexon signal (normalized to DAPI, ***p<0.001, Student's t-test). **C,** Mice implanted with GBM43 PDX glioma cells were treated 5 days later with either saline or MT via i.p. injection. Two days later, animals were IN treated with OV-loaded NSCs. The IN treatment was repeated twice at one-week intervals. The survival of animals was recorded and analyzed using the log-rank test (n=8-9 per group * p<0.05).

Fibrin glue forms a solid framework to which NSCs can adhere, counteracting the normal clearing activity of ciliated epithelium; the sealant was observed to delay the clearance of NSCs, albeit only for 6 h after inoculation. MT treatment of animals is known to temporally disrupt the olfactory epithelium [11, 12, 17] and was anticipated to increase the number of NSCs passing through the olfactory barrier. Interestingly, we found that MT is superior to fibrin glue in delaying clearance of NSCs from the nasal cavity for up to 24 h after administration, perhaps by slowing the efficient mucus production and the ciliated epithelial villi movements, in addition to known phenomenon of the thinning of the nasal barrier.

MT treatment has been shown to impact terminally differentiated epithelial cells primarily, while stem cells are largely preserved, allowing for regeneration [11, 12, 21]. The effect of dying epithelial cells on the local milieu remains to be elucidated. Aging epithelial cells are naturally shed into the nasal cavity and are replaced by new cells emerging from the basal layer of epithelium. The chemotactic activity of factors released from dying epithelial cells on NSCs migration from and within the nasal cavity has not been studied. It is also plausible to hypothesize that basal and horizontal stem-like cells rapidly replacing damaged epithelium [13] secrete soluble tropic factors to support the persistence and survival of NSCs within the nasal cavity. Dai et al. showed that the NOTCH signaling hub, also important for the function of NSC pools [22-24], mediates the recovery of olfactory epithelium after MT induced injury [25]. Confirmation of these mechanisms may allow for further enhancement of NSCs vitality and augment the targeted delivery of therapeutic agents to the brain.

We demonstrate that MT pretreatment led to the depletion of the nasal epithelium which opened a pathway for NSCs to traverse into the brain parenchyma before the epithelium regenerated. Our histology analysis confirmed that epithelial depletion is associated with the enhanced persistence of NSCs in the nasal cavity of mice that were treated with MT (Figure 2). Using quantitative high-resolution 3D MRI R2* maps, we demonstrate that SPIO-labeled NSCs accumulate throughout the glioma tissue regions significantly better after depletion of the epithelial barrier with MT (Figure 4). Furthermore, we were able to confirm enhanced penetration of NSCs to the brain and accumulation in tumor xenografts by utilizing NSCs expressing GFP (Figure 5). The ability to track the migration of SPIO labeled NSCs movements *in vivo,* longitudinally and quantitatively in three dimensions, provides a unique tool to accurately study the IN delivery efficiency of stem cells. It might also help to drive improvements in the therapy by providing insight into the timing of migration. Other clinically-relevant imaging modalities such as a single-photon emission computerized tomography (SPECT) or a positron emission tomography (PET) could be utilized for tracking stem cells. Recently, we have developed the SPECT-based technology for the analysis of stem cells migration within the brain using radiolabeled nanoparticles [26]. This approach can provide not only reliable quantitative measurements, but also visualize pathways IN-delivered stem cells utilize for movement from the nasal cavity to the brain.

In a recent clinical study, patients with incurable cancers, including GBM, were treated with MT along with 3,3',5-triiodo-L-thyronine for several weeks to induce hypothyroxinemia [27]. A significant improvement in actual versus expected survival was observed in 83% of patients (19 of 23 patients). Longer survival in the hypothyroid group of patients with recurrent GBM (10.1 months versus 3.1 months, p= 0.03) was observed in a recent phase I/II study [28]. Therefore, we first investigated if MT can induce a survival benefit in glioma-bearing mice. Our data demonstrate no survival advantage in MT-treated mice when compared with untreated control animals (Figure 3). However, unlike in clinical studies, our treatment regimen consisted only of a single dose of MT. IN treatment with NSCs-OV followed by disruption of olfactory epithelium resulted in significant improvement in the survival of animals bearing aggressive patient-derived glioma xenografts, in comparison to control animals. Our *in vitro* data also reveal that MT does not enhance the oncolytic activity of OV in glioma cells (Figure 3B). The therapeutic effect of NSCs-OV is likely due to a larger number of these cells reaching the tumor mass, as demonstrated by MRI (Figure 4) and quantification of the viral hexon protein (a measure of OV payload) within glioma tumor (Figure 6). Importantly, this survival benefit was achieved independently of any additive effect that may occur when this novel therapy is supplemented to the current standards of care. Limitations imposed by small rodent preclinical models include and not limited to: (i) anatomical differences in the nasal and olfactory systems between humans and mice discussed in more details in prior studies [14, 20]; (ii) inability of OV to replicate in murine glioma, thus limiting studies to mice bearing human xenograft tissue with deficient immune system; and (iii) using stem cells of human origin in mouse models of GBM. Nevertheless, our findings show exciting potential for clinical translation as they establish the platform strategy to deliver effective

therapies that bypass the BBB, and avoid the challenges associated with systemic therapy. Furthermore, this mode of therapy may be well-suited to address other brain tumor types with anatomical advantages, e.g. various skull base and sellar neoplasms.

Clinically, MT has a relatively mild side effect profile even with repeated administrations that last over months and years. The approach to transiently open up the nasal epithelial delivery pathway is a novel strategy which might have significant beneficial clinical implications in the context of GBM. Further refinement of this combined non-invasive IN administration and in vivo tracking (3D MRI) of NSCs migration can potentially allow for the increased efficiency and precision of these therapies at the clinical stage and might offer additive benefits to the current standard of care for inoperable tumors. As described earlier, stem cells administered intranasally take more than one path to neoplasms. This broadens their clinical applicability to tumors located in inoperable, vital regions such as the brain stem (pontine glioma). It is now established that stem cells can be loaded with therapeutic agents and directed to migrate to intracranial tumors [6, 8, 10]. However, to deliver therapeutically relevant doses of anti-cancer agent, we must continue to improve the efficiency of stem cell migration. Advanced *in vivo* imaging technologies can further provide insights into the spatiotemporal dynamics of NSCs behaviors. Future investigations can address the detailed physiological mechanisms underlying the impact of MT on nasal epithelium to enhance chemotaxis [14, 29]. To our knowledge, this report is the first attempt to improve intracranial NSCs migration through the manipulation of the nasal epithelial barrier, with *in vivo* imaging confirmation, *ex vivo* pathology validation, and survival benefit in rodent models of GBM.

Conclusions

The IN route of delivery for anti-tumor NSCs is proven suitable for GBM and has remarkable potential for translation to future therapies. However, this treatment modality is limited by the body's natural defenses that prevent entry through the nasal epithelium into the intracranial compartment. Although NSCs administered IN are still able to gain access to intracranial tumors, the fast clearance and olfactory epithelium barrier limit the efficacy of therapy. Pretreatment with MT temporarily depletes the nasal epithelium, reducing the clearance of NSCs and integrity of the barriers they must cross. As more NSCs are able to migrate to the tumor and deliver the therapeutic payload, improved survival of GBM-bearing mice is achieved, providing an encouraging platform for future development of non-invasive therapies to fight against malignant brain tumors.

Acknowledgements

This work was supported by NIH R01NS087990 (M.S.L. and I.V.B.) and P50CA221747 SPORE for Translational Approaches to Brain Cancer. Imaging work was performed at Northwestern University Center for Translational Imaging generously supported by the Department of Radiology and the Feinberg School of Medicine.

Competing Interests

The authors declare that there is no conflict of interest regarding the publication of this article.

References

1. Stupp R, Mason WP, van den Bent MJ, Weller M, Fisher B, Taphoorn MJ, Belanger K, Brandes AA, Marosi C, Bogdahn U et al. Radiotherapy plus concomitant and adjuvant temozolomide for glioblastoma. N Engl J Med. 2005; 352:987-996.
2. Liu G, Yuan X, Zeng Z, Tunici P, Ng H, Abdulkadir IR, Lu L, Irvin D, Black KL, Yu JS. Analysis of gene expression and chemoresistance of CD133+ cancer stem cells in glioblastoma. Mol Cancer. 2006; 5:67.
3. Wharton SB, McNelis U, Bell HS, Whittle IR. Expression of poly(ADP-ribose) polymerase and distribution of poly(ADP-ribosyl)ation in glioblastoma and in a glioma multicellular tumour spheroid model. Neuropathol Appl Neurobiol. 2000; 26:528-535.
4. Kozlovskaya L, Abou-Kaoud M, Stepensky D. Quantitative analysis of drug delivery to the brain via nasal route. J Control Release. 2014; 189:133-140.
5. Munster VJ, Prescott JB, Bushmaker T, Long D, Rosenke R, Thomas T, Scott D, Fischer ER, Feldmann H, de Wit E. Rapid Nipah virus entry into the central nervous system of hamsters via the olfactory route. Sci Rep. 2012; 2:736.
6. Reitz M, Demestre M, Sedlacik J, Meissner H, Fiehler J, Kim SU, Westphal M, Schmidt NO. Intranasal delivery of neural stem/progenitor cells: a noninvasive passage to target intracerebral glioma. Stem Cells Transl Med. 2012; 1:866-873.
7. Danielyan L, Schafer R, von Ameln-Mayerhofer A, Buadze M, Geisler J, Klopfer T, Burkhardt U, Proksch B, Verleysdonk S, Ayturan M et al. Intranasal delivery of cells to the brain. Eur J Cell Biol. 2009; 88:315-324.
8. Balyasnikova IV, Prasol MS, Ferguson SD, Han Y, Ahmed AU, Gutova M, Tobias AL, Mustafi D, Rincon E, Zhang L et al. Intranasal delivery of mesenchymal stem cells significantly extends survival of irradiated mice with experimental brain tumors. Mol Ther. 2014; 22:140-148.
9. Ahmed AU, Thaci B, Alexiades NG, Han Y, Qian S, Liu F, Balyasnikova IV, Ulasov IY, Aboody KS, Lesniak MS. Neural stem cell-based cell carriers enhance therapeutic efficacy of an oncolytic adenovirus in an orthotopic mouse model of human glioblastoma. Mol Ther. 2011; 19:1714-1726.
10. Yip S, Aboody KS, Burns M, Imitola J, Boockvar JA, Allport J, Park KI, Teng YD, Lachyankar M, McIntosh T et al. Neural stem cell biology may be well suited for improving brain tumor therapies. Cancer J. 2003; 9:189-204.
11. Xie F, Zhou X, Genter MB, Behr M, Gu J, Ding X. The tissue-specific toxicity of methimazole in the mouse olfactory mucosa is partly mediated through target-tissue metabolic activation by CYP2A5. Drug Metab Dispos. 2011; 39:947-951.
12. Fletcher RB, Prasol MS, Estrada J, Baudhuin A, Vranizan K, Choi YG, Ngai J. p63 regulates olfactory stem cell self-renewal and differentiation. Neuron. 2011; 72:748-759.
13. Kikuta S, Sakamoto T, Nagayama S, Kanaya K, Kinoshita M, Kondo K, Tsunoda K, Mori K, Yamasoba T. Sensory deprivation disrupts homeostatic regeneration of newly generated olfactory sensory neurons after injury in adult mice. J Neurosci. 2015; 35:2657-2673.
14. Dey M, Yu D, Kanojia D, Li G, Sukhanova M, Spencer DA, Pituch KC, Zhang L, Han Y, Ahmed AU et al. Intranasal Oncolytic Virotherapy with CXCR4-Enhanced Stem Cells Extends Survival in Mouse Model of Glioma. Stem Cell Reports. 2016; 7:471-482.
15. Dey M, Yu D, Kanojia D, Li G, Sukhanova M, Spencer DA, Pituch KC, Zhang L, Han Y, Ahmed AU et al. Intranasal Oncolytic Virotherapy with CXCR4-Enhanced Stem Cells Extends Survival in Mouse Model of Glioma. Stem Cell Reports. 2016; 7:471-482.
16. Jensen EC. Quantitative analysis of histological staining and fluorescence using ImageJ. Anat Rec (Hoboken). 2013; 296:378-381.

17. Leung CT, Coulombe PA, Reed RR. Contribution of olfactory neural stem cells to tissue maintenance and regeneration. Nat Neurosci. 2007; 10:720-726.
18. Portnow J, Synold TW, Badie B, Tirughana R, Lacey SF, D'Apuzzo M, Metz MZ, Najbauer J, Bedell V, Vo T et al. Neural Stem Cell-Based Anticancer Gene Therapy: A First-in-Human Study in Recurrent High-Grade Glioma Patients. Clin Cancer Res. 2017; 23:2951-2960.
19. Ahmed AU, Thaci B, Tobias AL, Auffinger B, Zhang L, Cheng Y, Kim CK, Yunis C, Han Y, Alexiades NG et al. A preclinical evaluation of neural stem cell-based cell carrier for targeted antiglioma oncolytic virotherapy. J Natl Cancer Inst. 2013; 105:968-977.
20. Harkema JR, Carey SA, Wagner JG. The nose revisited: a brief review of the comparative structure, function, and toxicologic pathology of the nasal epithelium. Toxicol Pathol. 2006; 34:252-269.
21. Dunn SJ, Fletcher AG, Chapman SJ, Gavaghan DJ, Osborne JM. Modelling the role of the basement membrane beneath a growing epithelial monolayer. J Theor Biol. 2012; 298:82-91.
22. Basak O, Giachino C, Fiorini E, Macdonald HR, Taylor V. Neurogenic subventricular zone stem/progenitor cells are Notch1-dependent in their active but not quiescent state. J Neurosci. 2012; 32:5654-5666.
23. Ghareghani M, Zibara K, Azari H, Hejr H, Sadri F, Jannesar R, Ghalamfarsa G, Delaviz H, Nouri E, Ghanbari A. Safflower Seed Oil, Containing Oleic Acid and Palmitic Acid, Enhances the Stemness of Cultured Embryonic Neural Stem Cells through Notch1 and Induces Neuronal Differentiation. Front Neurosci. 2017; 11:446.
24. Engler A, Rolando C, Giachino C, Saotome I, Erni A, Brien C, Zhang R, Zimber-Strobl U, Radtke F, Artavanis-Tsakonas S et al. Notch2 Signaling Maintains NSC Quiescence in the Murine Ventricular-Subventricular Zone. Cell Rep. 2018; 22:992-1002.
25. Dai Q, Duan C, Ren W, Li F, Zheng Q, Wang L, Li W, Lu X, Ni W, Zhang Y et al. Notch Signaling Regulates Lgr5(+) Olfactory Epithelium Progenitor/Stem Cell Turnover and Mediates Recovery of Lesioned Olfactory Epithelium in Mouse Model. Stem Cells. 2018; 36:1259-1272.
26. Cheng SH, Yu D, Tsai HM, Morshed RA, Kanojia D, Lo LW, Leoni L, Govind Y, Zhang L, Aboody KS et al. Dynamic In Vivo SPECT Imaging of Neural Stem Cells Functionalized with Radiolabeled Nanoparticles for Tracking of Glioblastoma. J Nucl Med. 2016; 57:279-284.
27. Hercbergs A, Johnson RE, Ashur-Fabian O, Garfield DH, Davis PJ. Medically induced euthyroid hypothyroxinemia may extend survival in compassionate need cancer patients: an observational study. Oncologist. 2015; 20:72-76.
28. Hercbergs AA, Goyal LK, Suh JH, Lee S, Reddy CA, Cohen BH, Stevens GH, Reddy SK, Peereboom DM, Elson PJ et al. Propylthiouracil-induced chemical hypothyroidism with high-dose tamoxifen prolongs survival in recurrent high grade glioma: a phase I/II study. Anticancer Res. 2003; 23:617-626.
29. Zhao D, Najbauer J, Garcia E, Metz MZ, Gutova M, Glackin CA, Kim SU, Aboody KS. Neural stem cell tropism to glioma: critical role of tumor hypoxia. Mol Cancer Res. 2008; 6:1819-1829.